

Hadronic Branching Fractions & $D\bar{D}$ Cross-sections at $\psi(3770)$ from CLEO-c

Yongsheng Gao (for CLEO Collaboration)*

Southern Methodist University, Dallas, Texas 75275-0175, USA

E-mail: gao@mail.physics.smu.edu

We present some recent results in hadronic decays and cross-section measurements at $\psi(3770)$ from CLEO Collaboration. They include measurement of absolute hadronic branching fractions of D mesons and $e^+e^- \rightarrow D\bar{D}$ cross sections, inclusive production of η , η' and ϕ in D decays, branching fractions of $D^+ \rightarrow K_{S,L}^0 \pi^+$ and $\eta \pi^+$, $\psi(3770)$ non- $D\bar{D}$ decays, and timelike electromagnetic form factors of pion, kaon, and proton. These results are based on 55.8 pb^{-1} and 281 pb^{-1} at $\psi(3770)$, and other data samples collected by the CLEO-c detector at the Cornell Electron Storage Ring (CESR).

*International Europhysics Conference on High Energy Physics
July 21st - 27th 2005
Lisboa, Portugal*

*Speaker.

1. Measurement of Absolute Hadronic Branching Fractions of D Mesons and

$e^+e^- \rightarrow D\bar{D}$ Cross Sections at $E_{\text{cm}} = 3773$ MeV

Absolute measurements of hadronic charm meson branching fractions play a central role in the study of the weak interaction because they serve to normalize many D and B meson branching fractions, from which elements of the Cabibbo-Kobayashi-Maskawa (CKM) matrix [1] are determined. For instance, the determination of the CKM matrix element $|V_{cb}|$ from the $B \rightarrow D^* \ell \nu$ decay rate using full D^* reconstruction requires knowledge of the D meson branching fractions [2, 3]. We present charge-averaged branching fraction measurements of three D^0 and six D^+ decay modes [4].

The data sample consists of 55.8 pb^{-1} of integrated luminosity collected by the CLEO-c detector on the $\psi(3770)$ resonance, at a center-of-mass energy $E_{\text{cm}} = 3773$ MeV. Reconstruction of one D or \bar{D} meson (called single tag or ST) tags the event as either $D^0\bar{D}^0$ or D^+D^- . For a given decay mode i , we measure independently the D and \bar{D} ST yields, denoted by N_i and \bar{N}_i . We determine the corresponding efficiencies, denoted by ε_i and $\bar{\varepsilon}_i$, from Monte Carlo simulations. Thus, $N_i = \varepsilon_i \mathcal{B}_i N_{D\bar{D}}$ and $\bar{N}_i = \bar{\varepsilon}_i \mathcal{B}_i N_{D\bar{D}}$, where \mathcal{B}_i is the branching fraction for mode i , assuming no CP violation, and $N_{D\bar{D}}$ is the number of produced $D\bar{D}$ pairs. Double tag (DT) events are the subset of ST events where both the D and \bar{D} are reconstructed. The DT yield for D mode i and \bar{D} mode j , denoted by N_{ij} , is given by $N_{ij} = \varepsilon_{ij} \mathcal{B}_i \mathcal{B}_j N_{D\bar{D}}$, where ε_{ij} is the DT efficiency. As with ST yields, the charge conjugate DT yields and efficiencies, N_{ji} and ε_{ji} , are determined separately. Charge conjugate particles are implied, unless referring to ST and DT yields.

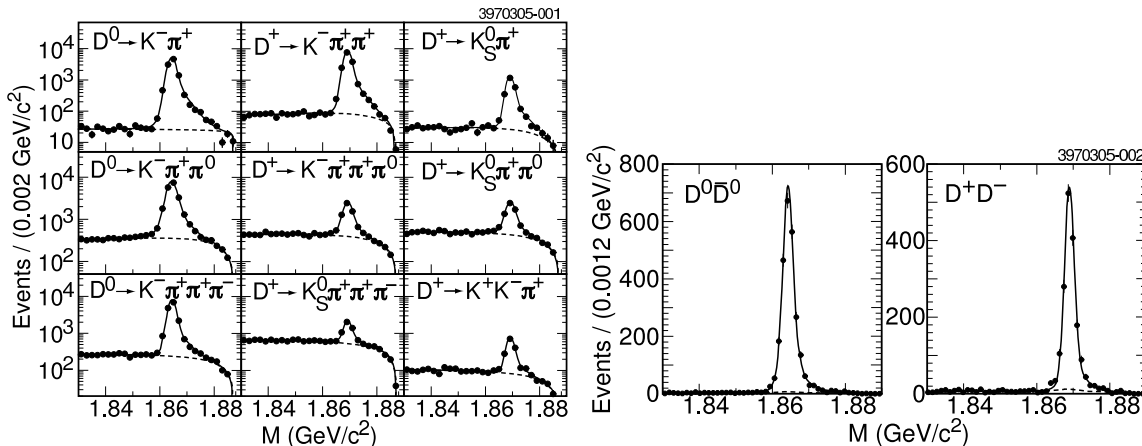


Figure 1: Left: Semilogarithmic plot of ST yields and fits for D and \bar{D} combined for each mode. Data are shown as points with error bars and the solid lines show the total fits and the dashed lines are the background shapes. The high mass tails on the signal are due to initial state radiation. Right: The DT yields and fits projected on the D^0 and D^+ axis summed over all modes. The solid lines show the total fit and the dashed lines the background shapes.

We extract branching fractions and $N_{D\bar{D}}$ by combining ST and DT yields with a least squares technique. We fit D^0 and D^+ parameters simultaneously, including in the χ^2 statistical and systematic uncertainties and their correlations for all experimental inputs [5]. Thus, yields, efficiencies, and backgrounds are treated uniformly, and the statistical uncertainties on \mathcal{B}_i and $N_{D\bar{D}}$ include the correlations among N_i , \bar{N}_j , and N_{ij} . Also, in the above efficiency ratios most systematic uncertain-

Table 1: Fitted branching fractions and $D\bar{D}$ pair yields, along with the fractional FSR corrections. Uncertainties are statistical and systematic, respectively. The Particle Data Group [3] lists the average branching fractions $\mathcal{B}(D^0 \rightarrow K^- \pi^+) = (3.85 \pm 0.09)\%$ and $\mathcal{B}(D^+ \rightarrow K^- \pi^+ \pi^+) = (9.1 \pm 0.7)\%$.

Parameter	Fitted Value	Δ_{FSR}
$N_{D^0\bar{D}^0}$	$(2.01 \pm 0.04 \pm 0.02) \times 10^5$	-0.2%
$\mathcal{B}(D^0 \rightarrow K^- \pi^+)$	$(3.91 \pm 0.08 \pm 0.09)\%$	-2.0%
$\mathcal{B}(D^0 \rightarrow K^- \pi^+ \pi^0)$	$(14.9 \pm 0.3 \pm 0.5)\%$	-0.8%
$\mathcal{B}(D^0 \rightarrow K^- \pi^+ \pi^+ \pi^-)$	$(8.3 \pm 0.2 \pm 0.3)\%$	-1.7%
$N_{D^+D^-}$	$(1.56 \pm 0.04 \pm 0.01) \times 10^5$	-0.2%
$\mathcal{B}(D^+ \rightarrow K^- \pi^+ \pi^+)$	$(9.5 \pm 0.2 \pm 0.3)\%$	-2.2%
$\mathcal{B}(D^+ \rightarrow K^- \pi^+ \pi^+ \pi^0)$	$(6.0 \pm 0.2 \pm 0.2)\%$	-0.6%
$\mathcal{B}(D^+ \rightarrow K_S^0 \pi^+)$	$(1.55 \pm 0.05 \pm 0.06)\%$	-1.8%
$\mathcal{B}(D^+ \rightarrow K_S^0 \pi^+ \pi^0)$	$(7.2 \pm 0.2 \pm 0.4)\%$	-0.8%
$\mathcal{B}(D^+ \rightarrow K_S^0 \pi^+ \pi^+ \pi^-)$	$(3.2 \pm 0.1 \pm 0.2)\%$	-1.4%
$\mathcal{B}(D^+ \rightarrow K^+ K^- \pi^+)$	$(0.97 \pm 0.04 \pm 0.04)\%$	-0.9%

Table 2: Ratios of branching fractions to the reference branching fractions $\mathcal{R}_0 \equiv \mathcal{B}(D^0 \rightarrow K^- \pi^+)$ and $\mathcal{R}_{\pm} \equiv \mathcal{B}(D^+ \rightarrow K^- \pi^+ \pi^+)$, along with the fractional FSR corrections. Uncertainties are statistical and systematic, respectively.

Parameter	Fitted Value	Δ_{FSR}
$\mathcal{B}(D^0 \rightarrow K^- \pi^+ \pi^0)/\mathcal{R}_0$	$3.65 \pm 0.05 \pm 0.11$	+1.2%
$\mathcal{B}(D^0 \rightarrow K^- \pi^+ \pi^+ \pi^-)/\mathcal{R}_0$	$2.10 \pm 0.03 \pm 0.06$	+0.3%
$\mathcal{B}(D^+ \rightarrow K^- \pi^+ \pi^+ \pi^0)/\mathcal{R}_{\pm}$	$0.613 \pm 0.013 \pm 0.019$	+1.7%
$\mathcal{B}(D^+ \rightarrow K_S^0 \pi^+)/\mathcal{R}_{\pm}$	$0.165 \pm 0.004 \pm 0.006$	+0.4%
$\mathcal{B}(D^+ \rightarrow K_S^0 \pi^+ \pi^0)/\mathcal{R}_{\pm}$	$0.752 \pm 0.016 \pm 0.033$	+1.4%
$\mathcal{B}(D^+ \rightarrow K_S^0 \pi^+ \pi^+ \pi^-)/\mathcal{R}_{\pm}$	$0.340 \pm 0.009 \pm 0.014$	+0.8%
$\mathcal{B}(D^+ \rightarrow K^+ K^- \pi^+)/\mathcal{R}_{\pm}$	$0.101 \pm 0.004 \pm 0.002$	+1.3%

ties are correlated between ST and DT efficiencies, so their effects largely cancel.

Figure 1 shows the M distributions for the nine decay modes with D and \bar{D} candidates combined. Overlaid are the fitted signal and background components. We also measure 45 DT yields in data and determine the corresponding efficiencies from simulated events. Figure 1 shows $M(D)$ for all modes combined, separated by charge. We find total DT yields of 2484 ± 51 for D^0 and 1650 ± 42 for D^+ .

The results of the data fit are shown in Table 1. We also compute ratios of branching fractions to the reference branching fractions, shown in Table 2. These ratios have higher precision than the individual branching fractions, and they also agree with the PDG averages. Without FSR corrections to the efficiencies, all seven ratios would be 0.3% to 1.7% higher. We obtain

Table 3: Single tag data yields and efficiencies and their background from the 281 pb⁻¹ data sample.

D Tag Mode	Yield	Background
$\bar{D}^0 \rightarrow K^+ \pi^-$	49418 ± 246	630
$\bar{D}^0 \rightarrow K^+ \pi^- \pi^0$	101960 ± 476	18307
$\bar{D}^0 \rightarrow K^+ \pi^- \pi^- \pi^+$	76178 ± 306	6421
$D^- \rightarrow K^+ \pi^- \pi^-$	77387 ± 281	1868
$D^- \rightarrow K^+ \pi^- \pi^- \pi^0$	24850 ± 214	12825
$D^- \rightarrow K_S^0 \pi^-$	11162 ± 136	514
$D^- \rightarrow K_S^0 \pi^- \pi^0$	20244 ± 170	170
$D^- \rightarrow K_S^0 \pi^- \pi^- \pi^+$	18176 ± 255	255

Table 4: Results of inclusive production of η , η' and ϕ in D decays from 281 pb⁻¹ data sample.

Mode	D^0 BR (%)	PDG (%)	D^+ BR (%)	PDG (%)
ηX	$9.4 \pm 0.4 \pm 0.6$	<13	$5.7 \pm 0.5 \pm 0.5$	<13
$\eta' X$	$2.6 \pm 0.2 \pm 0.2$	—	$1.0 \pm 0.2 \pm 0.1$	—
ϕX	$1.0 \pm 0.1 \pm 0.1$	1.7 ± 0.8	$1.1 \pm 0.1 \pm 0.2$	<1.8

the $e^+e^- \rightarrow D\bar{D}$ cross sections by scaling $N_{D^0\bar{D}^0}$ and $N_{D^+D^-}$ by the luminosity, which we determine to be $\mathcal{L} = (55.8 \pm 0.6) \text{ pb}^{-1}$. Thus, at $E_{\text{cm}} = 3773 \text{ MeV}$, we find peak cross sections of $\sigma(e^+e^- \rightarrow D^0\bar{D}^0) = (3.60 \pm 0.07^{+0.07}_{-0.05}) \text{ nb}$, $\sigma(e^+e^- \rightarrow D^+D^-) = (2.79 \pm 0.07^{+0.10}_{-0.04}) \text{ nb}$, $\sigma(e^+e^- \rightarrow D\bar{D}) = (6.39 \pm 0.10^{+0.17}_{-0.08}) \text{ nb}$, and $\sigma(e^+e^- \rightarrow D^+D^-)/\sigma(e^+e^- \rightarrow D^0\bar{D}^0) = 0.776 \pm 0.024^{+0.014}_{-0.006}$, where the uncertainties are statistical and systematic, respectively.

2. Inclusive Production of η , η' and ϕ in D Decays

Using 281 pb⁻¹ of full CLEO-c data at the $\psi(3770)$ resonance, we measure [6] inclusive production of η , η' and ϕ in D Decays. The tag yields are shown in Table 3. The measured inclusive branching fractions of η , η' and ϕ in D Decays, together with comparison with PDG, are shown in Table 4. They represent significant improvements comparing with current PDG measurements.

3. Measurements of $D^+ \rightarrow K_{S,L}^0 \pi^+$ and $\eta \pi^+$ Branching Fractions

Using the single charge D tag from 281 pb⁻¹ of CLEO-c data at $\psi(3770)$, we measure the branching fraction of $D^+ \rightarrow K_{S,L}^0 \pi^+$ using a missing mass technique: $\mathcal{B}(D^+ \rightarrow K_{S,L}^0 \pi^+) = (3.06 \pm 0.06 \pm 0.16)\%$, $\mathcal{B}(D^+ \rightarrow \eta \pi^+) = (0.39 \pm 0.03 \pm 0.03)\%$.

4. $\psi(3770)$ non- $D\bar{D}$ Decays

We also measure the branching fractions of $\psi(3770)$ to non- $D\bar{D}$ final states, including Vector-

Pseudoscalar and multi-body final states. The details of the event selections and results can be found in Ref. [7, 8].

5. Precision Measurements of the Timelike Electromagnetic Form Factors of Pion, Kaon, and Proton

Electromagnetic form factors of hadrons are among the most important physical observables. They provide direct insight into the distribution of charges, currents, color, and flavor in the hadron. Form factors for spacelike momentum transfers, $Q^2 > 0$, are determined by elastic scattering of electrons from hadrons available as targets. Form factors for timelike momentum transfers, $Q^2 < 0$, are measured by annihilation $e^+e^- \leftrightarrow h^+h^-$. They lead to insight into the wave function of the hadron in terms of its partonic constituents.

Using 20.7 pb^{-1} of e^+e^- annihilation data taken at $\sqrt{s} = 3.671 \text{ GeV}$ with the CLEO-c detector, we make precision measurements of the electromagnetic form factors of the charged pion, charged kaon, and proton for timelike momentum transfer of $|Q^2| = 13.48 \text{ GeV}^2$ by the reaction $e^+e^- \rightarrow h^+h^-$. The measurements [9] are the first ever with identified pions and kaons of $|Q^2| > 4 \text{ GeV}^2$, with the results $F_\pi(13.48 \text{ GeV}^2) = 0.075 \pm 0.008(\text{stat}) \pm 0.005(\text{syst})$ and $F_K(13.48 \text{ GeV}^2) = 0.063 \pm 0.004(\text{stat}) \pm 0.001(\text{syst})$. The result for the proton, assuming $G_E^p = G_M^p$, is $G_M^p(13.48 \text{ GeV}^2) = 0.014 \pm 0.002(\text{stat}) \pm 0.001(\text{syst})$, which is in agreement with earlier results.

References

- [1] M. Kobayashi and T. Maskawa, *Prog. Theor. Phys.* **49**, 652 (1973).
- [2] See review by M. Artuso and E. Barberio in Ref. [3].
- [3] Particle Data Group, S. Eidelman *et al.*, *Phys. Lett. B* **592**, 1 (2004).
- [4] CLEO Collaboration, Q. He *et al.*, *Phys. Rev. Lett.* **95**, 121801 (2005).
- [5] W.M. Sun, arXiv:physics/0503050, submitted to *Nucl. Instrum. Methods Phys. Res., Sec. A*.
- [6] CLEO Collaboration, M. Artuso *et al.*, CLEO CONF 05-4.
- [7] CLEO Collaboration, G.S. Adam *et al.*, CLEO CONF 05-1.
- [8] CLEO Collaboration, G.S. Huang *et al.*, CLNS 05/1921, CLEO 05-13.
- [9] CLEO Collaboration, T.K. Pedlar *et al.*, CLNS 05/1936, CLEO 05-24.